Time Dependence of Flow Patterns near the Convective Threshold in a Cylindrical Container

Guenter Ahlers and David S. Cannell
Department of Physics, University of California, Santa Barbara, California 93106

and

Victor Steinberg
Department of Nuclear Physics, The Weizmann Institute of Science, Rehovot 76100, Israel
(Received 6 February 1985)

Digitally processed shadowgraph images revealed time-dependent flow patterns slightly above the convective onset in a cylindrical cell of aspect ratio $L \equiv D/2d = 15.0$ (D is diameter, d is height). This time dependence was monitored for up to 200 horizontal thermal diffusion times. At larger Rayleigh numbers, the system reached time-dependent states after much shorter transients.

PACS numbers: 47.20.+m, 47.25.−c

A largely unresolved problem of great current interest is the prediction of the stability of patterns which form in many dissipative nonlinear systems driven far from equilibrium by an external stress. A well known example of such a system is Rayleigh-Bénard convection in a horizontal layer of fluid heated from below.[1,2] In that case, a stability analysis of the solutions of the equations of motion reveals that there should be stable, time-independent flow in the form of parallel, straight rolls near the convective threshold for the laterally infinite system.[3] Although real systems have sidewalls, it was widely assumed that systems of sufficiently large lateral extent would likewise exhibit time-independent flow states, at least near threshold. Thus, it came as a surprise when sensitive heat-flow measurements at cryogenic temperatures revealed nonperiodic time dependence in a cylindrical sample of aspect ratio $L \equiv D/2d$ (D = diameter, d = thickness of the fluid layer) equal to 57, even when the Rayleigh number R exceeded its convective threshold value R_c by only about 10%.[4,5] To our knowledge, there has been no satisfactory explanation of this time dependence,[6] although considerable theoretical progress has been made in recent years towards taking the influence of the boundaries into account.[7] However, there also has been no independent experimental confirmation of the unsteady flow near R_c.[8,9]

In this Letter we report computer-enhanced shadowgraph visualizations of convective-flow patterns in a cylindrical system with $L = 15.0$. For $R \gtrsim 1.18R_c$, we found steady flow patterns, but for R close to R_c the patterns were time dependent.[10] In one particular case ($R = 1.141R_c$), this time dependence was observed under steady external conditions for 200 horizontal thermal-diffusion times (about one month). During this run, there was no obvious change in the nature of the time dependence during the last 160 diffusion times.

Our apparatus and flow visualization procedure have been described elsewhere.[11] We used a cylindrical cell with $D = 8.36$ cm and Plexiglass sidewalls. The height was $d = 0.278$ cm, uniform to ± 0.0005 cm. The working fluid was water with a Prandtl number $\sigma = 5.7$; the cold-end temperature was 25.70 °C, stable to $\pm 10^{-3}$ °C, and the temperature difference at threshold was 3.866 °C. For this system, the horizontal diffusion time $t_h \equiv L^2 t_v = 3.33$ h, and $t_v \equiv d^2/\kappa = 53$ sec (κ is the thermal diffusivity). The heat current q

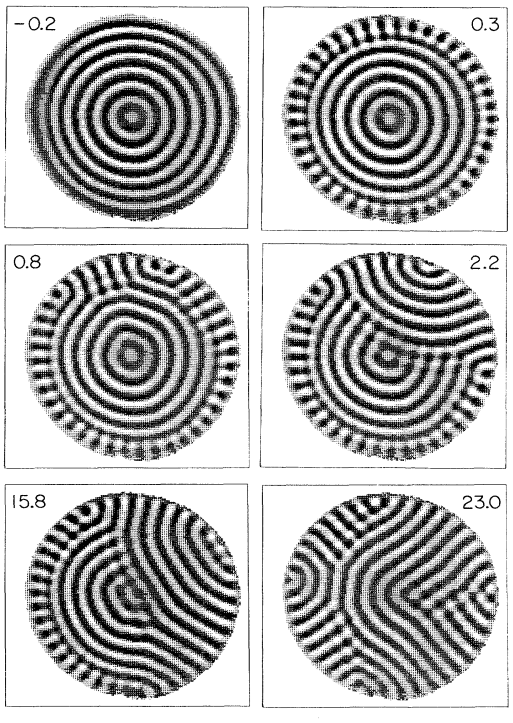

FIG. 1. Shadowgraph images of flow patterns. The number in each square is the elapsed time in units of the horizontal diffusion time since the pattern in the upper left corner was rendered unstable by changing the heat current from $1.39q_c$ to $1.30q_c$. This figure represents the early, transient stages of the pattern evolution. For $t > 0$, $\epsilon = 0.141$.

© 1985 The American Physical Society

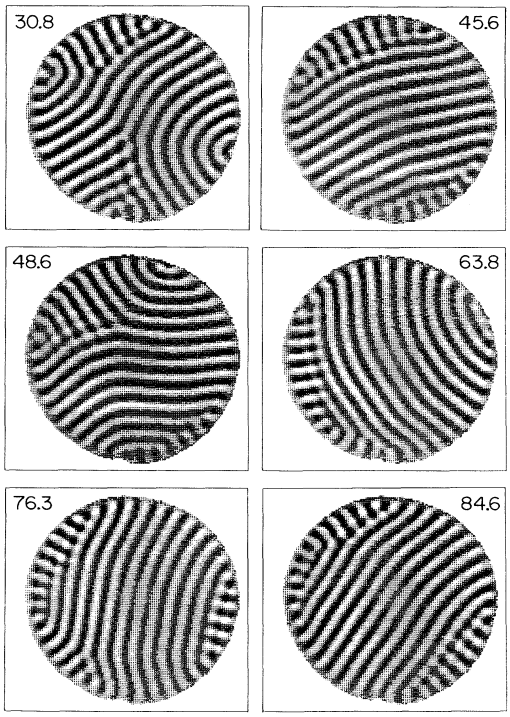

FIG. 2. Shadowgraph images for $\epsilon = 0.141$, as in Fig. 1, but for $30 \lesssim t \lesssim 85$.

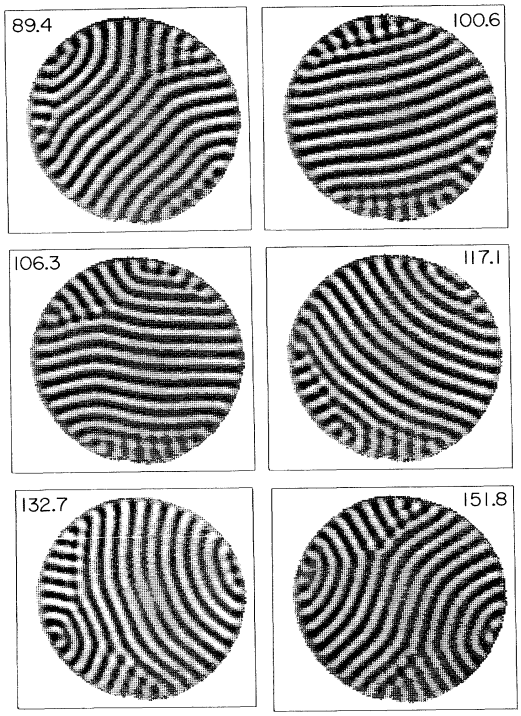

FIG. 3. Shadowgraph images for $\epsilon = 0.141$, as in Fig. 1, but for $85 \lesssim t \lesssim 160$.

was held constant to at least one part in 10^4, and, in the absence of convection, 96.6% of it was carried by the fluid. Shadowgraph images were taken at time intervals of $0.43 t_h$.

In Figs. 1 to 4 we show 24 images. The first, in the upper left corner of Fig. 1, represents the pattern of the initial state which was prepared at larger R as described elsewhere.[11] At the imposed heat current $q = 1.388 q_c$, it is stable in our cell and corresponds to $\epsilon \equiv R/R_c - 1 = 0.184$ (q_c is the current required to reach R_c in steady state). At $t = 0$, q was reduced to $1.295 q_c$. Within a few vertical diffusion times, this yielded $\epsilon = 0.141$, independent of time[12] to ± 0.001. The subsequent 23 images were taken at that current. The numbers in each square are the elapsed time since the change in q, in units of t_h.

The six images for $0 < t \lesssim 40$ show transient behavior involving relatively large and rapid changes associated with the breakup of the concentric rolls which existed for $t \leq 0$. Although of interest for their own sake, these transients are qualitatively different from the time dependence observed for $t \gtrsim 40$. The early-time evolution starts with cross-roll formation at the boundaries and then involves relatively complicated patterns often containing many defects. This interval, $0 < t \lesssim 40$, corresponds to the range over which others[9] have computed a Lyapunov functional from flow visualizations, mostly at larger ϵ than ours, and

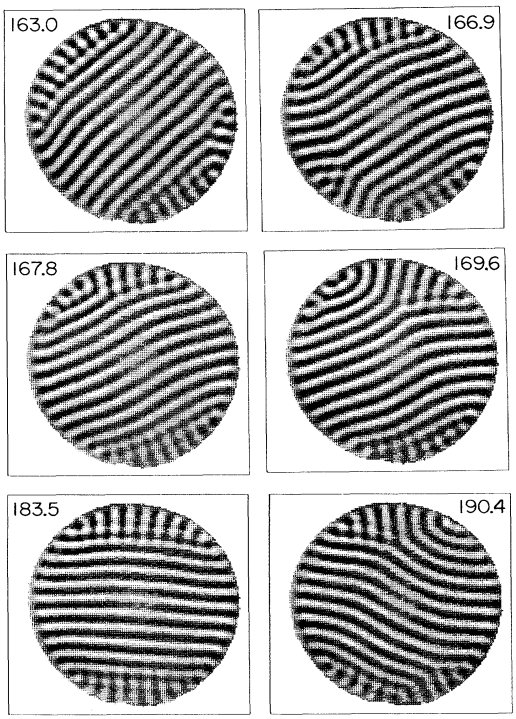

FIG. 4. Shadowgraph images for $\epsilon = 0.141$, as in Fig. 1, but for $160 \lesssim t \lesssim 200$.

have found this functional to be monotonically decreasing in time. We believe that it also corresponds to the duration of the slow transients reported on the basis of model calculations.[6]

For $t \gtrsim 40$, the patterns for the most part appear simpler than those in the early stages. They are, however, unequivocally time dependent,[10] and changes were always severe and rapid enough to be easily noticeable by casual inspection of patterns separated in time by, say, $4t_h$ (often changes were more rapid). A characteristic feature of this late-time evolution is the repeated establishment (albeit at seemingly random intervals) of patterns consisting primarily of nearly straight rolls terminating almost perpendicular to the boundary and of two defect combinations nearly on opposite sides of the cell. The defect combinations typically consisted primarily of a grain boundary. This type of pattern occurred for t near 45.6, 63.8, 84.6, 100.6, 117.1, 163.0, 167.8, and 183.5, and for those times is reproduced in Figs. 2 to 4. Each of the occurrences of this pattern type was separated from the previous and the next occurrence by the seemingly more complicated pattern type represented by images at $t=48.6$, 76.3, 89.4, 106.3, 132.7, 151.8, 166.9, 169.6, and 190.4 in Figs. 2 to 4. The latter patterns contained an additional grain boundary, typically of length $4d$ to $12d$, terminating with one end at the cell wall and the other in a disclination in the cell interior, as well as remnants of the two defect combinations on opposite sides. An example is shown in the upper right-hand section of the image at $t=169.6$ in Fig. 4. Sometimes two such disclination–grain-boundary combinations coexisted, as for instance at $t=151.8$ in Fig. 3. The transition from the relatively simpler to the apparently more complicated pattern always occurred by the new defect structure (i.e., the disclination–grain-boundary combination) splitting away from one of the two previously existing grain boundaries. Thereafter, the new defect combination would move along the circumference of the cell and be reabsorbed by one of the two main grain boundaries, usually on the side opposite to where it was created. The images in Figs. 2 to 4 show eight repetitions of this process at seemingly random intervals and rates. (The process is only approximately repetitive, and we do not mean to imply that exactly the same patterns are reformed.)

After the last image in Fig. 4 was taken, the current was changed in steps to $q=1.652q_c$, $2.066q_c$, $1.527q_c$, $1.388q_c$, $1.295q_c$, $1.205q_c$, and $1.295q_c$ in that sequence, corresponding in steady state to $\epsilon=0.304$, 0.493, 0.247, 0.183, 0.141, 0.098, and 0.141, respectively. At each step, images were obtained for a period of about $30t_h$ (about four days). In all but the last two cases, a time-dependent[10] pattern was formed. Four of these are reproduced in Fig. 5. For the last two power levels ($q=1.205q_c$ and $1.295q_c$) a time-dependent state similar to that shown in Figs. 2 to 4 was reestablished.

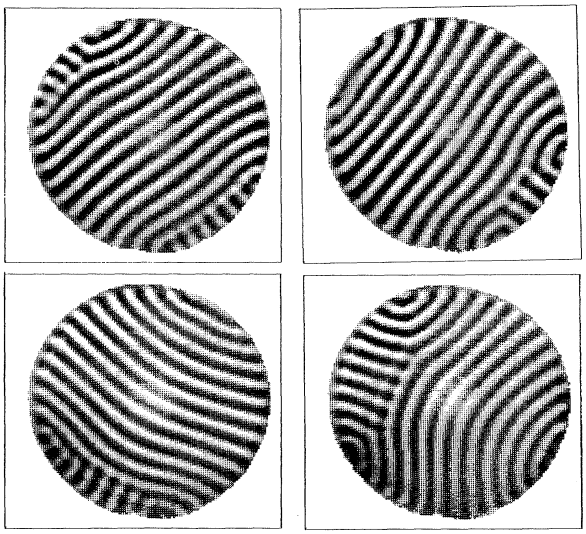

FIG. 5. Shadowgraph images of steady states reached for $\epsilon=0.304$ (upper left), 0.493 (upper right), 0.247 (lower left), and 0.183 (lower right). Although we call them steady (Ref. 10), these patterns rotate in a clockwise direction.

It is interesting to note that the pattern which had formed at $\epsilon=0.183$ (lower right of Fig. 5) remained nearly unchanged and stable when ϵ was decreased to 0.141 where time dependence had been observed earlier (Figs. 2 to 4). However, the small additional decrease of ϵ to 0.098 caused the nearly immediate decay of that pattern to one extremely similar, for instance, to that shown in Fig. 4 for $t=183.5$, and the time dependence was reestablished.

The measurements reported in this Letter reveal that Rayleigh-Bénard convection in a cylindrical container with $L=15$ and $\sigma=5.7$ is time dependent for ϵ of order 0.1. Clearly, many additional experiments involving months and perhaps years are required in order to determine the influence of L, σ, boundary symmetry, and possibly thermal history on the range of existence and the nature of this time dependence near the convective onset in a fluid heated from below.

We are grateful to Christopher Meyer for his help in this experiment. This work was supported by the National Science Foundation through Grant No. MEA81-17241.

[1]Lord Rayleigh, Philos. Mag. **32**, 529 (1916).

[2]H. Bénard, Rev. Gen. Sci. Pure Appl. **11**, 1261, 1309 (1900), and Ann. Chim. Phys. **23**, 62 (1901).

[3]A. Schlüter, D. Lortz, and F. Busse, J. Fluid Mech. **23**,

129 (1965).

[4]G. Ahlers and R. P. Behringer, Phys. Rev. Lett. **40**, 712 (1978), and Prog. Theor. Phys. Suppl. **64**, 186 (1978).

[5]R. P. Behringer and G. Ahlers, J. Fluid Mech. **125**, 219 (1982).

[6]Greenside and co-workers [H. S. Greenside, W. M. Coughran, Jr., and N. L. Schryer, Phys. Rev. Lett. **49**, 726 (1982); H. S. Greenside and W. M. Coughran, Jr., Phys. Rev. A **30**, 398 (1984)], on the basis of numerical calculations using model equations, have shown that surprisingly long transients (much longer than t_h) are involved in the adjustments of their model flow patterns. We believe that similar transients could explain the large changes during the first $40t_h$ of the present experiment. We think it unlikely that they explain the observed time dependence up to $200t_h$.

[7]See, for instance, M. C. Cross, Phys. Rev. A **25**, 1065 (1982), and references therein.

[8]Experiments by Gollub and co-workers [J. P. Gollub and J. F. Steinman, Phys. Rev. Lett. **47**, 505 (1981); J. P. Gollub, A. R. McCarrier, and J. F. Steinman, J. Fluid Mech. **125**, 259 (1982)] on the flow evolution in a rectangular container at larger values of R than those explored here usually yielded steady flow patterns. Very recent work by M. S. Heutmaker, P. N. Fraenkel, and J. P. Gollub, preceding Letter [Phys. Rev. Lett. **54**, 1369 (1985)], on pattern evolution in a cylindrical container has provided some evidence consistent with the long-time behavior reported here.

[9]Heutmaker, Fraenkel, and Gollub, Ref. 8.

[10]We use a somewhat qualitative definition of time dependence. We will ignore rotation of the pattern as a whole, which was usually observed when there was no line of reflection symmetry. We will also not concern ourselves with minor wave-number adjustments, the detection of which would require quantitative measurements. Instead, we will call a pattern time dependent only if obvious, qualitative changes occurred over time intervals of a few horizontal diffusion times.

[11]V. Steinberg, G. Ahlers, and D. S. Cannell, Phys. Scr. (to be published).

[12]Even though the pattern changes in Figs. 1 to 4 are very dramatic, we find that the heat transport is not influenced strongly by these changes. However, our experiment does not have the resolution to detect the very small noise amplitude measured in the cryogenic experiment (Refs. 4 and 5).

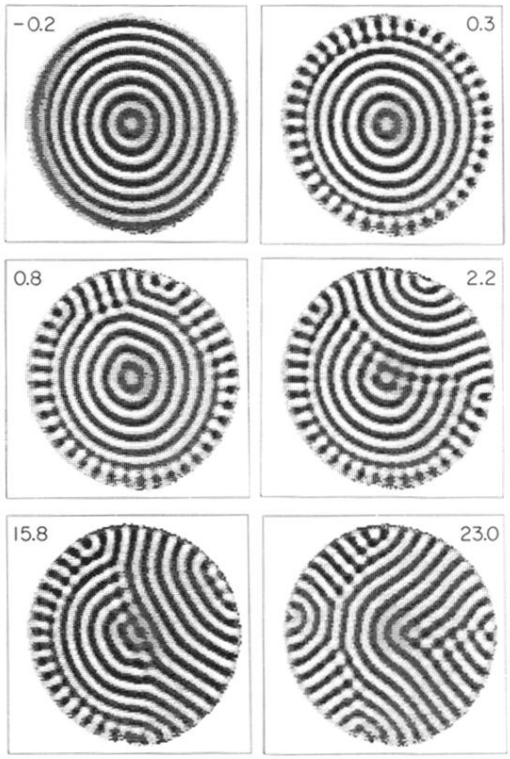

FIG. 1. Shadowgraph images of flow patterns. The number in each square is the elapsed time in units of the horizontal diffusion time since the pattern in the upper left corner was rendered unstable by changing the heat current from $1.39q_c$ to $1.30q_c$. This figure represents the early, transient stages of the pattern evolution. For $t > 0$, $\epsilon = 0.141$.

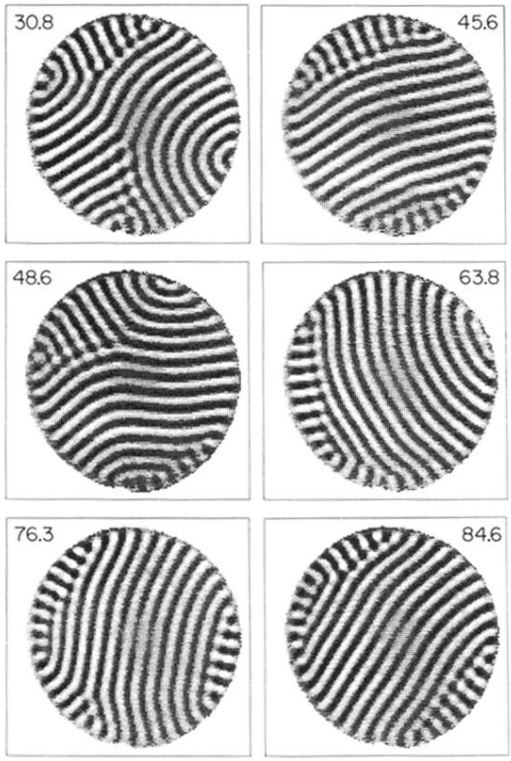

FIG. 2. Shadowgraph images for $\epsilon = 0.141$, as in Fig. 1, but for $30 \lesssim t \lesssim 85$.

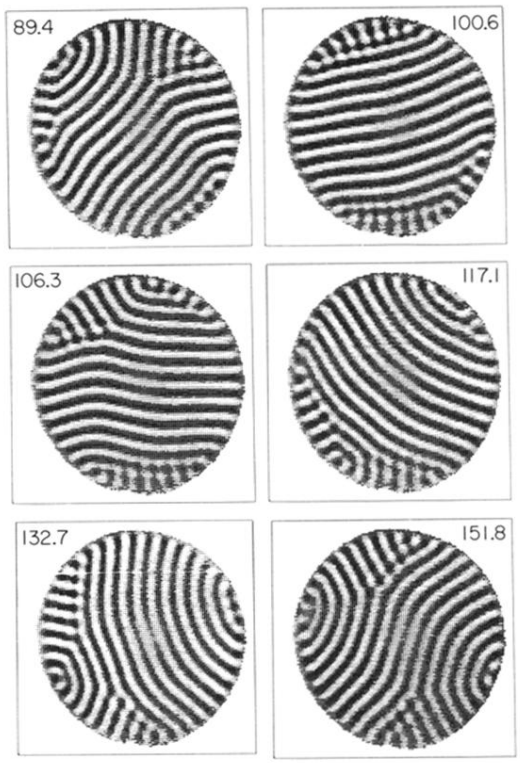

FIG. 3. Shadowgraph images for $\epsilon = 0.141$, as in Fig. 1, but for $85 \lesssim t \lesssim 160$.

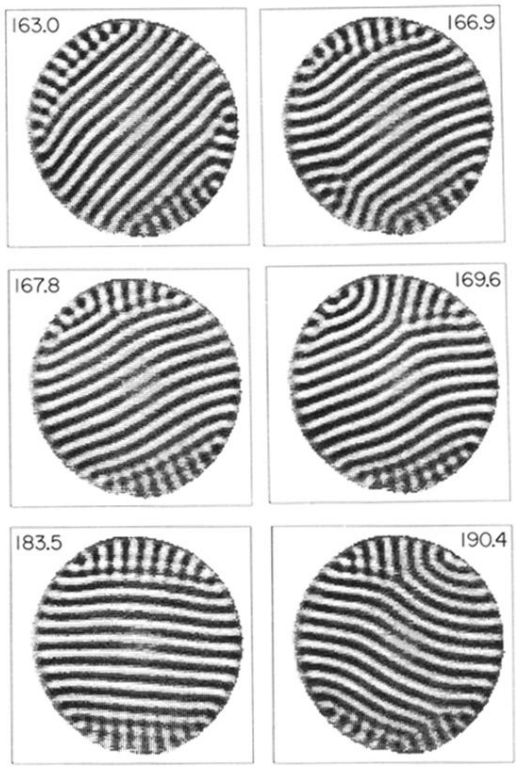

FIG. 4. Shadowgraph images for $\epsilon = 0.141$, as in Fig. 1, but for $160 \lesssim t \lesssim 200$.

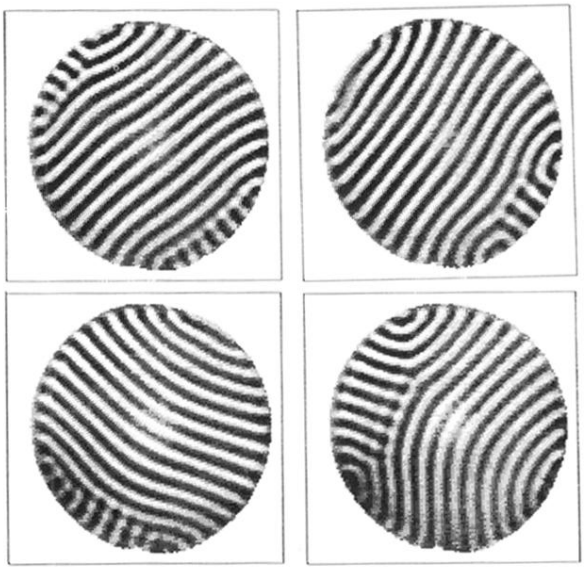

FIG. 5. Shadowgraph images of steady states reached for $\epsilon = 0.304$ (upper left), 0.493 (upper right), 0.247 (lower left), and 0.183 (lower right). Although we call them steady (Ref. 10), these patterns rotate in a clockwise direction.